AIAA Journal
Vol. 50, No. 2, February 2012

Study of Turbulence–Radiation Interaction in Hypersonic Turbulent Boundary Layers

L. Duan* and M. P. Martín†
University of Maryland, College Park, Maryland 20742
A. M. Feldick‡
Pennsylvania State University, University Park, Pennsylvania 16802
M. F. Modest§
University of California, Merced, Merced, California 95344
and
D. A. Levin¶
Pennsylvania State University, University Park, Pennsylvania 16802

DOI: 10.2514/1.J051247

Direct numerical simulations are conducted to investigate the effect of turbulence–radiation interaction in hypersonic turbulent boundary layers, representative of the Orion crew exploration vehicle at the peak heating condition during reentry. Both the effects of emission and absorption are considered by solving the radiative transfer equation using the tangent slab approximation and a spectral model with line-by-line accuracy. Nondimensional governing parameters to measure the significance of turbulence–radiation interaction are proposed, and the direct numerical simulation fields with and without radiation coupling are used to assess turbulence–radiation interaction. Is it found that the fluid medium within the boundary layer is optically thick with local emission largely counterbalanced by the absorbed irradiation, which results in much weaker overall radiative source term $\nabla \cdot \mathbf{q}_R$, and the thermal radiation has minimal backward influence on the turbulence flowfield. In addition, both the uncoupled and coupled results show that there is no sizable interaction between turbulence and radiation at the hypersonic environment under investigation. An explanation for small turbulence–radiation interaction intensity is also provided.

Nomenclature

A	=	total absorption, W/m^3
H	=	shape factor, δ^*/θ, dimensionless
h	=	specific enthalpy, J/kg
M	=	Mach number, dimensionless
n	=	number density, m^{-3}
q	=	turbulence kinetic energy, $(u'^2 + v'^2 + w'^2)/2$, m^2/s^2
$\mathbf{q}_R$	=	radiative heat flux, W/m^3
Re_θ	=	Reynolds number, $\equiv \rho_\delta u_\delta \theta/\mu_\delta$, dimensionless
$Re_{\delta 2}$	=	Reynolds number, $\equiv \rho_\delta u_\delta \theta/\mu_w$, dimensionless
Re_τ	=	Reynolds number, $\equiv \rho_w u_\tau \delta/\mu_w$, dimensionless
T	=	temperature, K
u	=	streamwise velocity, m/s
u_τ	=	friction velocity, m/s
v	=	spanwise velocity, m/s
w	=	wall-normal velocity, m/s
δ	=	boundary-layer thickness, m
δ^*	=	displacement thickness, m
ε	=	total emission, W/m^3
ϵ	=	dissipation rate, m^2/s^3
θ	=	momentum thickness, m
λ	=	wavelength, m
μ	=	mixture viscosity, $kg/(m \cdot s)$
ρ	=	density, kg/m^3

Subscripts

s	=	chemical species
w	=	wall variables
x, y, z	=	streamwise, spanwise, and wall-normal directions for spatial coordinates
δ	=	boundary-layer edge
λ	=	at a given wavelength

Superscript

$+$	=	inner-wall units

Presented as Paper 2011-749 at the 49th AIAA Aerospace Sciences Meeting, Orlando, FL, 4–7 January 2011; received 23 February 2011; revision received 22 July 2011; accepted for publication 25 July 2011.

*Visiting Graduate Student, Department of Aerospace Engineering; currently National Institute of Aerospace, Hampton, VA 23666. Member AIAA.

†Associate Professor, Department of Aerospace Engineering. Associate Fellow AIAA.

‡Graduate Student, Department of Mechanical Engineering. Student Member AIAA.

§Shaffer and George Professor of Engineering, School of Engineering. Associate Fellow AIAA.

¶Professor, Department of Aerospace Engineering. Associate Fellow AIAA.

I. Introduction

THERMAL radiation has long been recognized to contribute significantly to the overall heat load [1] for spacecraft during entry into planetary atmospheres or Earth return, which typically has velocities exceeding 10 km/s. The radiative heat load onto such vehicles comes from both the radiation within the boundary layer, as well as the transmission of external radiation hitting the boundary layer. Turbulence in the boundary layer influences radiation, referred to as turbulence–radiation interaction (TRI), either by raising or lowering the transmissivity of radiation from the shock layer (absorption TRI) or by increasing emission from within the boundary layer (emission TRI).

The few previous studies on TRI for hypersonic turbulent boundary layers had been carried out using turbulent flowfields either without radiation coupling or those coupled with simplified radiation models. For example, Feldick et al. [2] evaluated the effects of absorption TRI in the form of boundary-layer absorption of radiation emitted in the shock layer using uncoupled direct numerical simulation (DNS) fields, under conditions typical of the Orion crew exploration vehicle (CEV) during reentry. They found that the effects of absorption TRI are minimal, although a slight decrease in boundary-layer transmissivities is predicted. Under similar conditions, Duan et al. [3] assessed emission TRI using coupled and uncoupled DNS fields. They used the optically thin assumption to avoid modeling spectral dependencies and reduce the required computational time. With the optically thin assumption, only the local emission from within the boundary layer has been considered while the boundary-layer absorption of radiation has been neglected. They found that TRI due to local emission within the boundary layer only subtly increases total emission and has negligible influence on mean flow quantities (mean temperature and velocity) as well as turbulent kinetic energy, but significantly enhances the effect of reducing temperature fluctuations and total emission fluctuations. Although previous studies provide important insights on how radiation gets augmented due to turbulence and are essential for isolating and characterizing the separate influences of turbulence on emission and absorption, a complete characterization of TRI in hypersonic boundary layers, taking into account the boundary-layer absorption of radiation emitted both locally within the boundary layer and in the shock layer, has not yet been explored.

In the current work, we provide a complete characterization of TRI in hypersonic turbulent boundary layers by conducting DNS fully coupled with radiation including both emission and absorption. With the fully coupled spectrally accurate solution obtained, the effects of TRI in hypersonic turbulent boundary layers are assessed under conditions typical of Orion CEV during reentry. The paper is structured as follows. The flow conditions and simulation details are given in Sec. III. The details of radiation modeling are introduced in Sec. IV. The nondimensional governing parameter for estimating TRI is given in Sec. IV. Results are given in Sec. V. Finally, conclusions are given in Sec. VI.

II. Flow Conditions and Simulation Details

We consider the boundary layer for Orion CEV, which enters the Earth's atmosphere at 9.5 km/s, at an altitude of 53 km, and angle of 18 deg. These conditions represent Earth entry at peak heating. Table 1 shows the boundary-layer edge conditions and wall parameters for the DNS. The simulation details, including the governing equations, constitutive relations, numerical methods, and initial and boundary conditions, are described in Duan et al. [3]. The calculations of the radiative heat flux are introduced in Sec. III. Table 2 gives the domain size ($L_x \times L_y \times L_z$), the grid size ($\Delta x \times \Delta y \times \Delta z$), and the number of grid points ($N_x \times N_y \times N_z$) for various DNS cases (listed in Table 3). Grid convergence studies have been conducted for all cases.

Table 1 Dimensional boundary-layer edge and wall parameters for direct numerical simulations

Parameter	Value
M_δ	0.153
ρ_δ	0.011 kg/m^3
T_δ	9622 K
T_w	2607 K
Re_θ	73
Re_τ	314
$Re_{\delta 2}$	214
θ	4.0 mm
H	0.1
δ	23.5 mm

III. Radiation Modeling

A. Radiative Transport Equation Solution

The radiative source term at each wavelength $(\nabla \cdot \mathbf{q}_R)_{s\lambda}$ is governed by the radiative transport equation (RTE) and can be formulated as [4]

$$(\nabla \cdot \mathbf{q}_R)_{s\lambda} = 4\pi\varepsilon_{s\lambda} - \kappa_{s\lambda} \int_{4\pi} I_\lambda \, \mathrm{d}\Omega \tag{1}$$

where $\varepsilon_{s\lambda}$ and $\kappa_{s\lambda}$ is the spectral emission and absorption coefficients, respectively, I_λ is the spectral intensity and Ω is the solid angle. Equation (1) states that physically the net loss of radiative energy from a control volume is equal to emitted energy minus absorbed irradiation. In addition, it is a spectral relation, i.e., it gives the divergence of heat flux per unit wavelength at a certain spectral position. If the total heat flux is desired, Eq. (1) needs to summed over all species and integrated over the entire spectrum to give

$$\nabla \cdot \mathbf{q}_R = \sum_s \int_0^\infty \left(4\pi\varepsilon_{s\lambda} - \kappa_{s\lambda} \int_{4\pi} I_\lambda \, \mathrm{d}\Omega\right) \mathrm{d}\lambda \tag{2}$$

In the current study, a one-dimensional tangent slab RTE solver [5] is used to calculate the radiative source term at each wavelength $(\nabla \cdot \mathbf{q}_R)_{s\lambda}$, which is then summed over all species and integrated in wavelength space to produce a total integrated source term $\nabla \cdot \mathbf{q}_R$. The tangent slab approximation makes use of the property that for hypersonic shock layers the radiative flux does not vary greatly in the body-tangential direction and assumes that radiation is effectively one-dimensional ($\nabla \cdot \mathbf{q}_R \doteq \mathrm{d}q/\mathrm{d}z$). The RTE is solved in one-dimensional columns, with each column being approximated by a series of one-dimensional infinite parallel plates [4]. The development of the tangent slab solver and its validation has been discussed in detail in Feldick et al. [5].

B. Spectral Modeling

Accurate modeling of emission and absorption coefficient spectra for radiating species ($\varepsilon_{s\lambda}$, $\kappa_{s\lambda}$) are necessary for calculating the radiation field. During typical Earth reentry conditions, the diatomic species in the flow around the spacecraft may become highly dissociated and emission from the two atomic species N and O, including bound–bound, bound–free, and free–free transitions, is the major source of radiation from the shock layer. The atomic species are treated with the multigroup full-spectrum correlated k distribution of Bansal et al. [6,7], taking advantage of the narrowband k-distribution databases for N and O, which make on-the-fly full-spectrum k-distribution spectral properties more efficient [8].

In the development of the spectrum correlated-k-distribution method for atoms in nonequilibrium plasmas, Bansal et al. [6,7] neglected the overlap between N and O species, which was found to be a valid assumption [8,9]. In contrast, overlap between atomic

Table 2 Grid resolution and domain size for various DNS cases[a]

Case	L_x/δ	L_y/δ	L_z/δ	Δx^+	Δy^+	z_2^+	α	N_x	N_y	N_z
I	9.5	1.9	8.7	47.4	9.6	0.55	1.11	64	64	60
II	9.5	1.9	8.7	47.4	9.6	0.55	1.11	64	64	60
III	9.5	1.9	8.7	47.4	9.6	0.55	1.11	64	64	60

[a]Uniform grid spacings are used in the streamwise and spanwise directions with constant Δx^+ and Δy^+. Geometric stretching is used in the wall-normal direction, with $z_k = z_2(\alpha^{k-1} - 1)/(\alpha - 1)$.

Table 3 DNS cases

Case	Radiative heat flux
I	$\nabla \cdot \mathbf{q}_R = 0$
II	$\nabla \cdot \mathbf{q}_R = (T, n_s)$
III	$\nabla \cdot \mathbf{q}_R = (\bar{T}, \bar{n}_s)$

radiation and molecular bands may be important for some cases, particularly in the vacuum-ultraviolet (VUV) part of the spectrum. Overlap between species is treated with a multiscale k-distribution model [10] for gas mixtures in thermodynamic nonequilibrium. It was found that overlap between different species is not important in the wavelength range greater than 1750 Å, due to the optically thin nature of molecular bands. For this spectral range a gray model was applied for molecular bands, and the full-spectrum k-distribution method was used to treat the atomic species. In the VUV region there is strong absorption by bands of N_2. In the k-distribution model the RTEs are solved separately for each emitting species and overlap with other species is treated in an approximate way. The spectral overlap between species is calculated such that the exact transmissivity of a homogeneous gas layer is recovered. This mixing model is coupled with the narrowband k-distribution database and atomic continuum database to allow efficient determination of the overlap factor and solution of the RTE in nonequilibrium and nonhomogeneous gas mixtures, following Bansal et al. [10].

IV. Governing Parameters for TRI

The difference between $\overline{\nabla \cdot \mathbf{q}_R(T, n_s)}$ and $\nabla \cdot \mathbf{q}_R(\bar{T}, \bar{n}_s)$ is a measure of TRI intensity and indicates how thermal radiation gets augmented due to turbulent fluctuation. To further predict how such augmentation effects influence the overall turbulence flowfield, we propose the nondimensional parameters based on order-of-magnitude analysis.

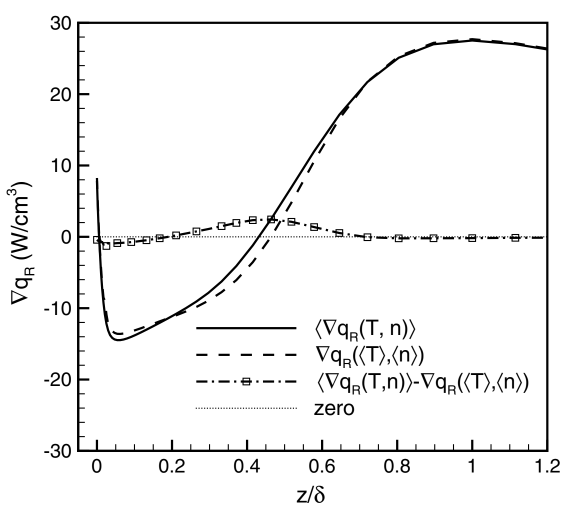

Fig. 1 Turbulent and laminar radiative source term $\nabla \cdot \mathbf{q}_R$ across the boundary layer for DNS case I.

Thermal radiation acts as a source/sink of energy in the total energy equation. The influence of thermal radiation on the turbulence flowfield can be estimated by the radiative heat ratio $\overline{\Delta h}$, defined as

$$\overline{\Delta h} \equiv \frac{\nabla \cdot \mathbf{q}_R(\bar{T}, \bar{n}_s)\tau_t}{\sum_{i=1}^{ns} \bar{\rho}_i (h_i(\bar{T}) + \frac{1}{2}\bar{u}_k \bar{u}_k)} \tag{3}$$

where τ_t is some characteristic turbulence time scale, the choice of which may be large-eddy turnover time δ/U_δ or q/ϵ, which is the time scale for energy-containing eddies. $\overline{\Delta h}$ is the ratio of radiative heat gain/loss during the characteristic turbulence flow time to the total flow enthalpy and provides a measure of the relative importance of thermal radiation to the overall turbulence flowfield. If the magnitude of $\overline{\Delta h}$ is close to or larger than unity, a significant change in flowfield by thermal radiation is expected.

By the same token, to estimate the enhanced heat gain/loss due to TRI, we introduce interaction radiative heat ratio $\overline{\Delta h^I}$, which is defined as

$$\overline{\Delta h}^I \equiv \frac{(\overline{\nabla \cdot \mathbf{q}_R(T, n_s)} - \nabla \cdot \mathbf{q}_R(\bar{T}, \bar{n}_s))\tau_t}{\sum_{i=1}^{ns} \bar{\rho}_i (h_i(\bar{T}) + \frac{1}{2}\bar{u}_k \bar{u}_k)} \tag{4}$$

where $\overline{\nabla \cdot \mathbf{q}_R(T, n_s)} - \nabla \cdot \mathbf{q}_R(\bar{T}, \bar{n}_s)$ is included to provide a measure for the intensity of TRI. The interaction radiative heat ratio is the ratio of enhanced heat gain/loss due to TRI during the characteristic flow time to the total flow enthalpy and provides a measure of the relative importance of TRI to the overall turbulence flowfield. If the magnitude of $\overline{\Delta h^I}$ is close to or larger than unity, a significant change in flowfield by TRI is expected.

Similar order-of-magnitude analyses have been performed by Martín and Candler [11,12] and Duan and Martín [13] in the study of turbulence–chemistry interaction as well as by Duan et al. [3] in the study of emission TRI.

V. Results

To investigate the effects of TRI, we perform three different DNS cases, as listed in Table 3. In case I, radiation is uncoupled to the flow with $\nabla \cdot \mathbf{q} = 0$. In case II, radiation is fully coupled to the turbulent flowfield, with the RTE solver introduced in Sec. III. In case III, radiation is included, but calculated based only on the mean flow quantities, excluding the interaction between turbulence and radiation.

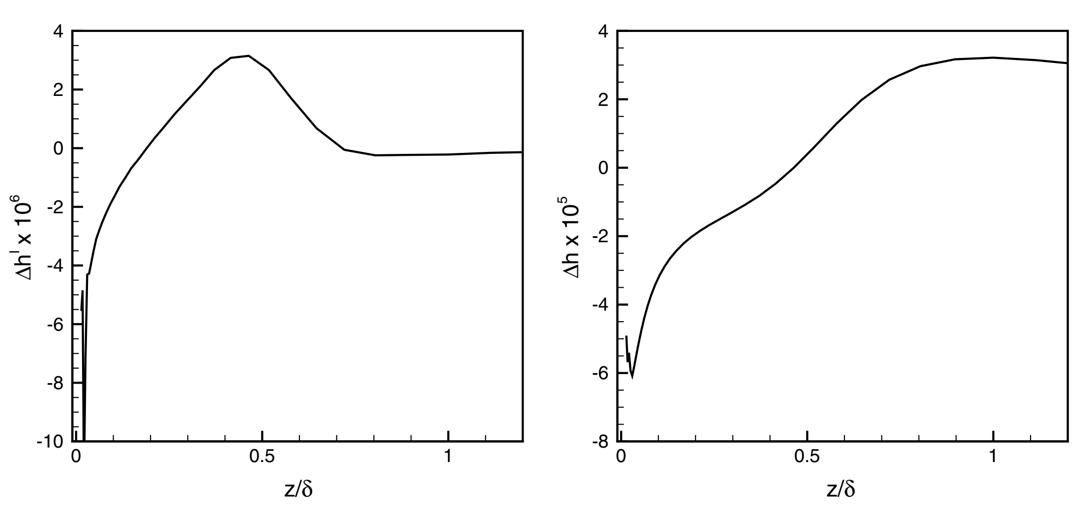

Fig. 2 a) Interaction radiative heat ratio $\overline{\Delta h^I}$, defined by Eq. (4), and b) radiative heat ratio $\overline{\Delta h}$, defined by Eq. (3), across the boundary layer for DNS case I. In the calculation, τ_t is chosen to be large-eddy turnover time.

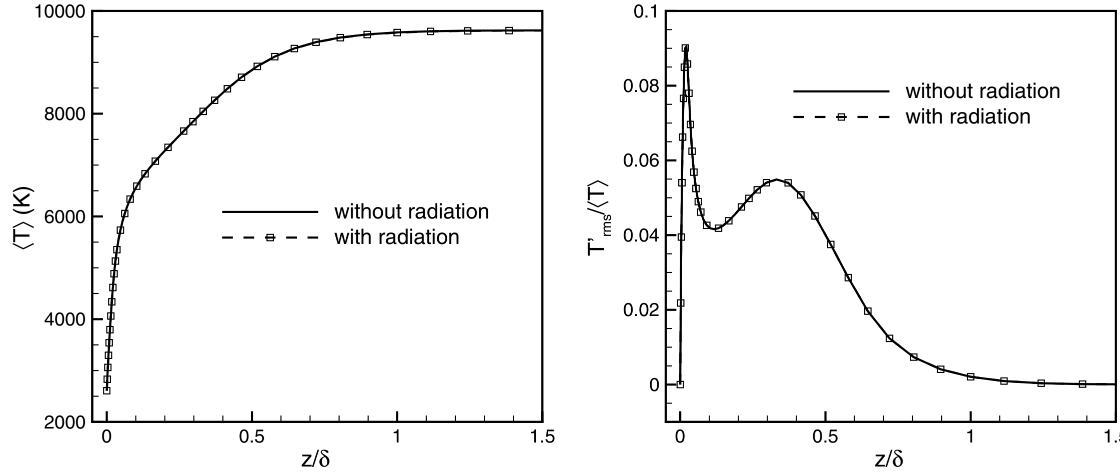

a) b)

Fig. 3 Mean and rms of temperature for DNS case I (without radiation) and case II (with radiation).

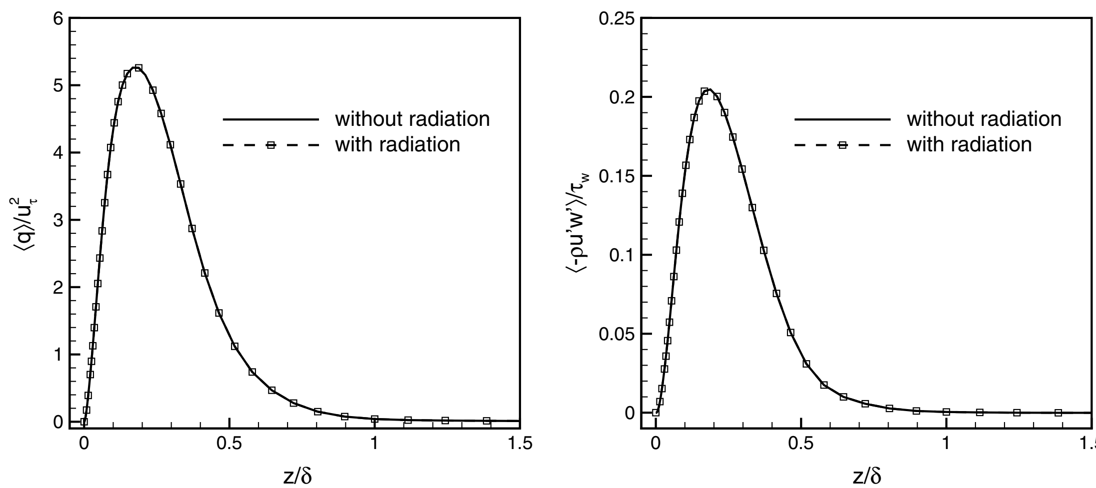

a) b)

Fig. 4 a) Turbulent kinetic energy and b) Reynolds shear stress for DNS case I (without radiation) and case II (with radiation).

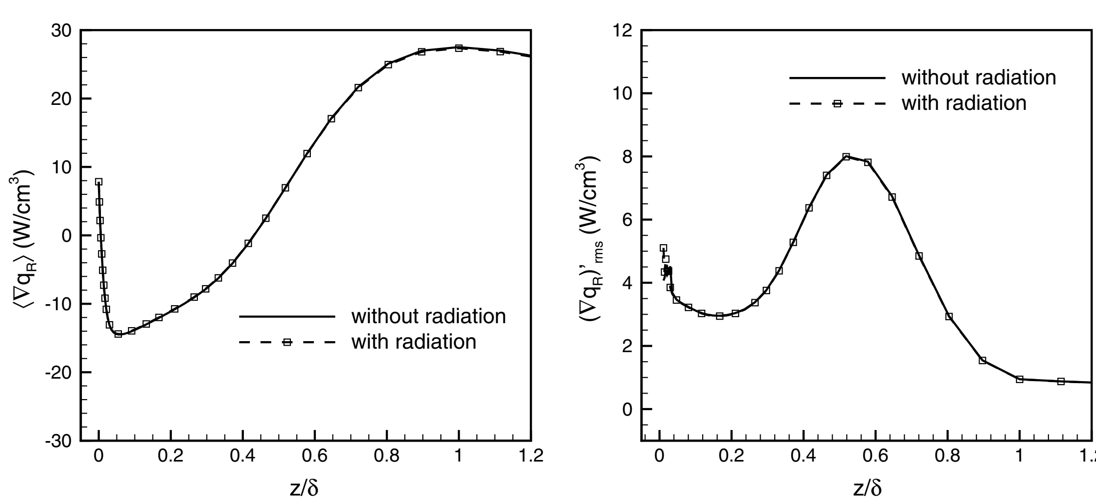

a) b)

Fig. 5 Mean and rms of radiative source term $\nabla \cdot \mathbf{q}_R$ for DNS case I (without radiation) and case II (with radiation).

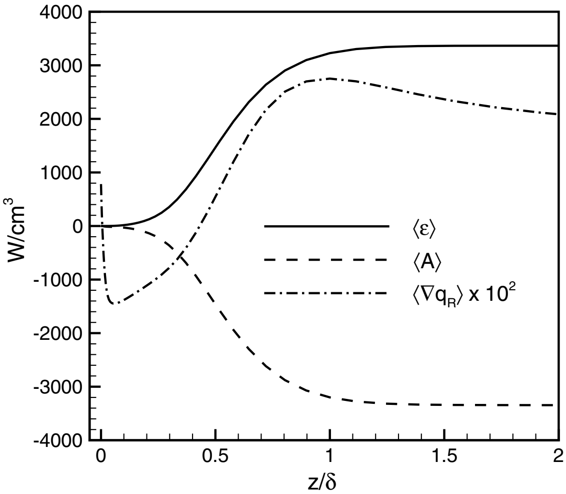

Fig. 6 Total emission $\bar{\varepsilon}$, absorption $\bar{A}$, and radiative source term $\overline{\nabla \cdot \mathbf{q}_R}$ across the boundary layer for DNS case II.

For the results shown in this section, averages are computed over streamwise and spanwise directions for each field; then an ensemble average is calculated over fields spanning approximately $120\delta^*/U_\delta$. The average of f over the x and y directions will be denoted by $\bar{f}$ or $\langle f \rangle$, and fluctuations about this mean will be denoted by f'.

A. DNS Without Radiation Coupling

TRI is first assessed using DNS fields without radiation coupling (case I), which neglects the backward influence of radiation on the flow. The DNS fields are similar to those used by Duan et al. [3] to investigate how total emission gets augmented due to turbulent fluctuation.

To investigate the influence of turbulent fluctuations on radiative source term $\nabla \cdot \mathbf{q}$, Fig. 1 plots $\overline{\nabla \cdot \mathbf{q}(T, n_s)}$ and $\nabla \cdot \mathbf{q}(\bar{T}, \bar{n}_s)$ across the boundary layer. It is shown that although the maximum relative difference between the turbulent and laminar radiative source terms may become large in regions where $\nabla \cdot \mathbf{q}(\bar{T}, \bar{n}_s)$ is small, the absolute difference remains small and is within ± 3 W/cm^3 all through the boundary layer. The turbulent and laminar wall-directed radiative heat fluxes $\overline{q_w(T, n_s)}$ and $q_w(\bar{T}, \bar{n}_s)$ are also similar with values 252.3 and 251.5 W/cm^2, respectively.

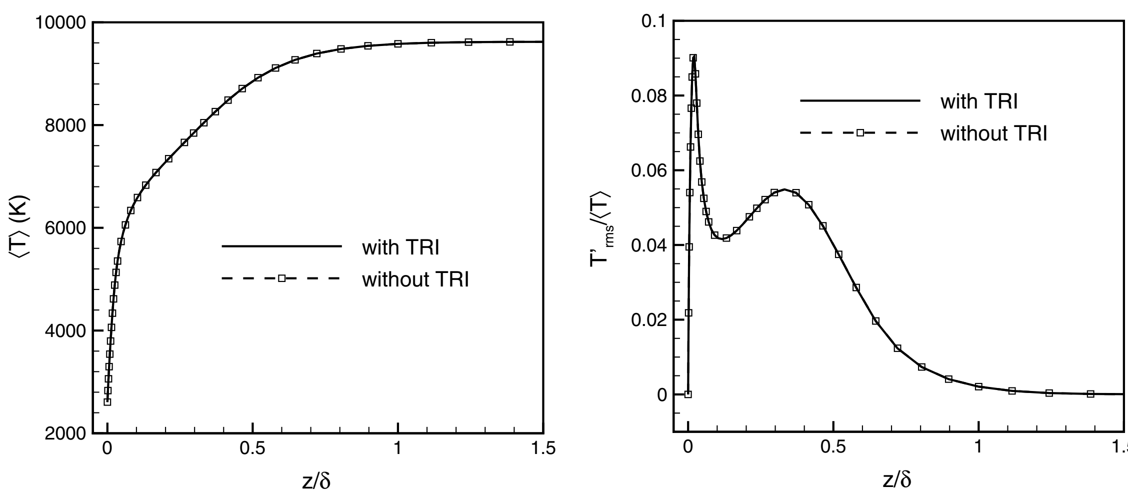

a) b)

Fig. 7 Mean and rms of temperature for DNS case II (with TRI) and case III (without TRI).

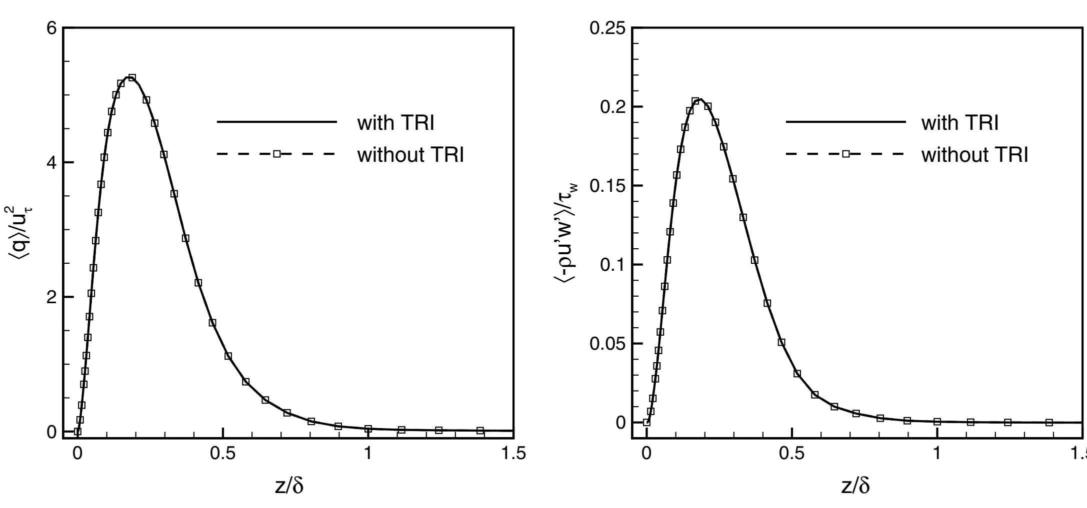

a) b)

Fig. 8 a) Turbulent kinetic energy and b) Reynolds shear stress for DNS case II (with TRI) and case III (without TRI).

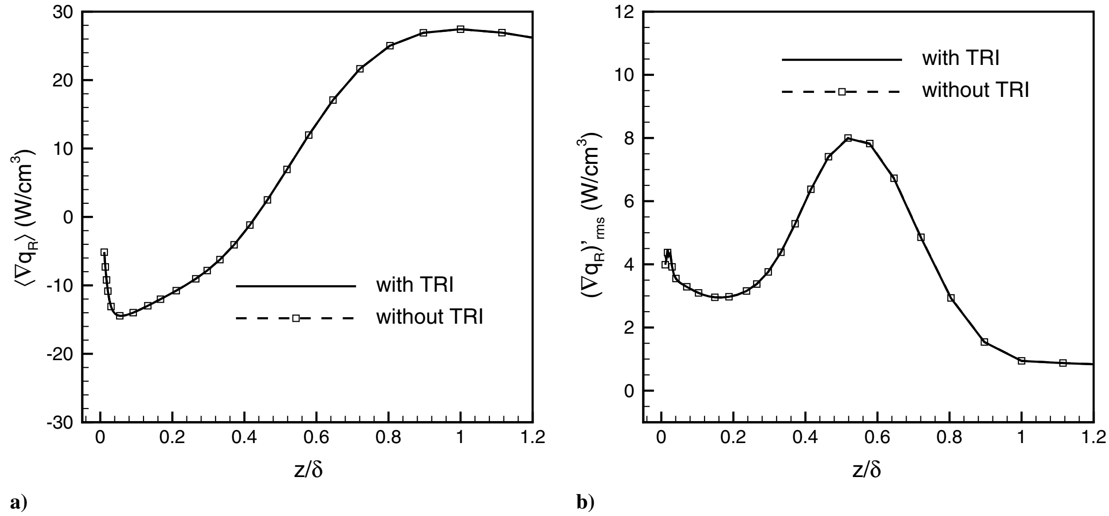

Fig. 9 Mean and rms of radiative source term for DNS case II (with TRI) and case III (without TRI).

To predict the effect of TRI on the turbulence flowfield, Fig. 2a plots the interaction radiative heat ratio [defined by Eq. (4)]. It is shown that $\overline{\Delta h^I}$ is more than 5 orders of magnitude smaller than unity, indicating that the enhanced heat gain/loss due to TRI has little influence on the turbulence flowfield.

The assessment of TRI using uncoupled DNS flowfields can be justified by Fig. 2b, which shows that the radiative heat ratio $\overline{\Delta h}$ [defined by Eq. (3)] is also significantly smaller than unity, indicating minimal backward influence of radiation on the turbulence flowfield.

B. DNS with Radiation Coupling

We further study the influence of radiation on the turbulence flowfield as well as assess TRI by coupling radiation to the flow solver (cases II and III).

First, the backward influence of thermal radiation on the turbulence flowfield is investigated by comparing DNS results with and without radiation coupling (cases I and II). Figure 3 shows that thermal radiation has negligible influences on both the mean temperature and temperature fluctuations. Figures 4 and 5 further show that thermal radiation hardly influences the turbulent kinetic energy, the Reynolds shear stress, and the radiative source term. The negligible difference between coupled and uncoupled results is consistent with the small value of $\overline{\Delta h}$.

The minimal influence of radiation on the turbulence flowfield is different from the observations by Duan et al. [3], who found significant reduction in both flow temperature and temperature fluctuations under similar flow conditions after only the emission is introduced (assuming $\nabla \cdot \mathbf{q} = \varepsilon$). In reality, however, the net radiative energy change for a given fluid element comes from both emission and absorption (i.e., $\nabla \cdot \mathbf{q} = \varepsilon + A$). For the current boundary-layer flow, the thermal emission within the boundary layer is largely counterbalanced by the absorbed irradiation from the shock layer, as indicated by Fig. 6, which shows that the magnitude of $\nabla \cdot \mathbf{q}_R$ is more than 2 orders of magnitude smaller than that of ε. As a result, the influence of overall thermal radiation on the turbulence flowfield becomes much weaker.

Next, the intensity of TRI is assessed by comparing results with and without TRI (cases II and III). Consistent with the small value of $\overline{\Delta h^I}$, Figs. 7–9, show negligible differences in various flow quantities between cases II and III, indicating minimal intensity of TRI.

The insignificant influence of TRI on the turbulent flow dynamics for hypersonic boundary layers is different from that found for many combustion flows, as described in Sec. I. In the study of emission TRI in hypersonic turbulent boundary layers, Duan et al. [3] argue that the possible reason for the difference is that under typical Earth reentry conditions, the atomic species such as N and O are the strongest radiators [14]. The generation of these radiating species requires the reaction of air, which happens at significantly higher temperatures ($T > 2500$ K) than those for typical combustion applications. The significantly higher flow enthalpy required to initialize the air reactions overwhelms the enhanced heat gain/loss due to TRI. The current study further confirms this argument, as indicated in Fig. 2.

VI. Conclusions

Direct numerical simulations were conducted of turbulent boundary layers to study turbulence–radiation interaction, using conditions typical of Orion crew exploration vehicle at peak heating during reentry. DNS fields with and without radiation coupling are considered.

The uncoupled results show that turbulent fluctuations have only subtle influence on the radiative source term and wall-directed radiative heat flux, and the coupled results show that thermal radiation as well as TRI have minimal backward influence on the overall turbulence flowfield at the hypersonic environment under investigation. Both the uncoupled and coupled results demonstrate that the nondimensional governing parameters ($\overline{\Delta h}$ and $\overline{\Delta h^I}$), which are derived based on the order-of-magnitude analysis, provide good metrics for estimating the relative importance of thermal radiation and TRI.

Acknowledgments

This work is sponsored by NASA Constellation University Institutes Project (CUIP) grant no. NCC3-989. We thank Peter Gnoffo for insightful discussions and the Entry Systems and Technology Division at NASA Ames Research Center for providing Reynolds-averaged Navier–Stokes solutions under flow conditions representative of crew exploration vehicles.

References

[1] Whiting, E. E., and Park, C., "Radiative Heating at the Stagnation Point of the AFE Vehicle," NASA TM 102829, 1990.

[2] Feldick, A., Duan, L., Modest, M., Martín, M., and Levin, D., "Influence of Interactions Between Turbulence and Radiation on Transmissivities in Hypersonic Turbulent Boundary Layers," AIAA Paper 2010-1185, 2010.

[3] Duan, L., Martín, M. P., Sohn, I., Levin, D., and Modest, D., "Study of Emission Turbulence–Radiation Interaction in Hypersonic Turbulent Boundary Layers," *AIAA Journal*, Vol. 49, No. 2, 2011, pp. 340–348. doi:10.2514/1.J050508

[4] Modest, M. F., *Radiative Heat Transfer*, 2nd ed., Academic Press, New York, 2003.

[5] Feldick, A. M., Modest, M. F., and Levin, D. A., "Closely Coupled Flowfield-Radiation Interaction for Flowfields Created During Hypersonic Reentry," AIAA Paper 2008-4104, 2008.

[6] Bansal, A., Modest, M. F., and Levin, D. A., "Correlated-*k* Distribution Method for Atomic Radiation in Hypersonic Nonequilibrium Flows," 47th AIAA Aerospace Sciences Conference, AIAA Paper 2009-1027, 2009.
[7] Bansal, A., Modest, M. F., and Levin, D. A., "Narrow-Band *k*-Distribution Database for Atomic Radiation in Hypersonic Nonequilibrium Flows," *ASME Summer Heat Transfer Conference*, ASME Paper HT2009-88120, 2009.
[8] Bansal, A., Modest, M. F., and Levin, D. A., "Correlated-*k* Distribution Method for Atomic Radiation in Hypersonic Nonequilibrium Flows," *Journal of Thermophysics and Heat Transfer* (to be published).
[9] Bansal, A., Modest, M. F., and Levin, D. A., "Narrow-Band *k*-Distribution Database for Atomic Radiation in Hypersonic Nonequilibrium Flows," *Journal of Heat Transfer* (submitted for publication).
[10] Bansal, A., Modest, M. F., and Levin, D. A., "*k*-Distributions for Gas Mixtures in Hypersonic Nonequilibrium Flows," 48th AIAA Aerospace Sciences Meeting, AIAA Paper 2010-234, 2010.
[11] Martín, M. P. and Candler, G. V., "Effect of Chemical Reactions on Decaying Isotropic Turbulence," *Physics of Fluids*, Vol. 10, No. 7, 1998, pp. 1715–1724.
doi:10.1063/1.869688
[12] Martín, M. P., and Candler, G. V., "Subgrid-Scale Model for the Temperature Fluctuations in Reacting Hypersonic Turbulent Flows," *Physics of Fluids*, Vol. 11, No. 9, 1999, pp. 2765–2771.
doi:10.1063/1.870135
[13] Duan, L., and Martín, M. P., "Assessment of Turbulence–Chemistry Interaction in Hypersonic Turbulent Boundary Layers," *AIAA Journal*, Vol. 49, No. 1, 2011, pp. 172–184.
doi:10.2514/1.J050605
[14] Ozawa, T., Wang, A., Modest, M. F., and Levin, D. A., "Particle Methods for Simulating Atomic Radiation in Hypersonic Reentry Flows," *AIP Conference Proceedings*, Vol. 1084, American Inst. of Physics, Melville, NY, 2008, pp. 748–753.

T. Jackson
Associate Editor